

A novel fluorogenic probe for visualizing the hydrogen peroxide in Parkinson's disease models

Gaobin Zhang*, Zheng Li[†], Fangjie Chen*, Duoteng Zhang[†], Wenhui Ji[†], Zhengpeng Yang*,
Qiong Wu^{†,§,||}, Chengwu Zhang[†], Lin Li^{†,¶,||} and Wei Huang^{†,‡}

*Henan Key Laboratory of Materials on Deep-Earth Engineering
School of Materials Science and Engineering
Henan Polytechnic University
Jiaozuo 454003, Henan, P. R. China

[†]Key Laboratory of Flexible Electronics (KLOFE)
& Institute of Advanced Materials (IAM)
Nanjing Tech University (NanjingTech)
30 South Puzhu Road
Nanjing 211816, P. R. China

[‡]Shaanxi Institute of Flexible Electronics (SIFE)
Northwestern Polytechnical University (NPU)
127 West Youyi Road, Xi'an 710072, P. R. China
[§]iamqwu@njtech.edu.cn
[¶]iamlli@njtech.edu.cn

Received 18 January 2020

Accepted 30 March 2020

Published 30 April 2020

Parkinson's disease (PD) is closely related to the oxidative stress induced by excess hydrogen peroxide (H_2O_2) in organisms. Developing an efficient method for noninvasive and real-time H_2O_2 detection is beneficial to investigate the role played by H_2O_2 in PD. In this work, a novel fluorogenic probe (CBH) for living organisms H_2O_2 detection has been designed, synthesized and characterized. The emission of CBH in PBS solution is very weak. However, when H_2O_2 was added, the fluorescence of CBH solution was sharply increased for 12-fold, accompanied by the emission peak blue-shifted from 600 to 530 nm. Moreover, the response of CBH to H_2O_2 is highly sensitive and selective and is not affected by various ROS/RNS, anions, cations, and amino acids. Based on the good performance of CBH for H_2O_2 detection, it has been successfully applied to visualizing the H_2O_2 concentration in living cells, Zebrafish and *C. elegans* PD models.

Keywords: Fluorescence; chemosensor; hydroperoxide; Parkinson's disease.

^{||}Corresponding authors.

This is an Open Access article. It is distributed under the terms of the Creative Commons Attribution 4.0 (CC-BY) License. Further distribution of this work is permitted, provided the original work is properly cited.

1. Introduction

As a well-known term for chemical species produced upon incomplete reduction of oxygen, reactive oxygen species (ROS) plays a key role in regulating various physiological functions of living organisms.^{1,2} The intrinsic biochemical properties of ROS underlie the mechanisms necessary for the development of living organisms. While, overproduction of ROS could give rise to oxidative stress that is implicated in plenty of diseases such as cancer, neurodegenerative diseases and inflammation,^{3–6} due to its paramount significance to ROS, hydrogen peroxide (H_2O_2) has been verified to affect cell growth, host defense, immune response, and signaling pathways.⁷ Parkinson's disease (PD) as a common neurodegenerative disorder in the elderly population mainly affects the motor system, and thus results in bradykinesia, rigidity, resting tremor, and postural instability.^{8,9} Although the etiology of PD is largely unknown, emerging studies have shown that the excess of ROS such as H_2O_2 causing oxidative stress inside cells is closely connected to PD.^{10,11} To reveal the fundamental roles of ROS, particularly H_2O_2 in PD living organisms, the real-time, noninvasive and high selective monitoring of H_2O_2 *in vivo* is highly desired.

Compared to other analytical methods, fluorescent probes meet the requirements of high sensitivity, selectivity, noninvasive and real-time detection analysis, and therefore they are regarded as a suitable method to monitor biomolecules and biological parameters in living systems.^{12–17} Recently, many fluorescence probes with outstanding performance for imaging H_2O_2 *in vivo* have been developed.^{18–21} For instance, Lin *et al.* presented a ratiometric probe for near-infrared (NIR) imaging of H_2O_2 in mitochondria based on the Baeyer–Villiger oxidative rearrangement reaction and reported a dual-response fluorescent probe for H_2O_2 and viscosity detection with different imaging channels.^{22,23} Peng *et al.* developed a two-photon NIR fluorescent turn-on probe for H_2O_2 based on dicyanomethylene-4H-pyran fluorophore, which can be used for endogenous and exogenous H_2O_2 two-photon NIR imaging.²⁴ However, challenges on high selective and fast response of imaging agents and desired photophysical properties lead to little research been done on the real-time imaging of H_2O_2 in living PD models.²⁵ Our group aims at developing high performance fluorescent dyes/probes for

imaging the PD related markers for the early diagnosis and therapy of the disease.^{26–31} We have reported some high-efficiency fluorescence probes for imaging H_2O_2 in PD models. For example, a mitochondria-targeted two-photon fluorogenic probe for the dual-imaging of viscosity and H_2O_2 levels in PD models were reported.³² A ratiometric NIR fluorogenic probe for visualizing H_2O_2 was developed, utilizing an excited-state intramolecular proton transfer strategy in PD models.³³ Nevertheless, all these probes were used in PD cell or *Drosophila* models. *Caenorhabditiselegans* (*C. elegans*) is the first model organism to have its entire genome sequenced. About 42% of *C. elegans* genes are related to human diseases and a few homologous chromosomes could be found in *C. elegans* for human diseases caused by genetic factors.³⁴ Moreover, hermaphrodite *C. elegans* have a simple but complete dopamine nervous system that exhibits the same characteristics as those of humans.³⁵ These features make *elegans* a suitable PD model. Although *C. elegans* are transparent, fluorogenic probes for detecting H_2O_2 in PD *C. elegans* model are rarely reported.

Herein, a novel fluorogenic probe (CBH) for living organisms H_2O_2 detection have been designed and synthesized. As shown in Scheme 1, the probe was synthesized in a simple way and benzeneboronic to be used for reaction site. The structure of the probe was characterized by ^1H and ^{13}C NMR. It could sensitively and selectively respond to H_2O_2 . The emission of CBH was very weak. However, a strong fluorescence signal appeared after the probe reacting with H_2O_2 in solution. Since CBH displayed good performance in H_2O_2 detection, it was successfully applied to monitor the H_2O_2 concentration in living cells, Zebrafish and *C. elegans* PD models.

2. Experimental

2.1. Materials and instrumentation

All chemical reactions were carried out under dry nitrogen protection atmosphere. All reagents and solvents were purchased from commercial suppliers directly, and they were used with no further purification unless otherwise noted. Reaction progress was monitored by thin-layer chromatography (TLC) on pre-coated silica plates (250 μm thickness) and spots were visualized by UV light. Silica

gel 60 (200–300 mesh, Silicycle) was for the column chromatography usage. ^1H and ^{13}C NMR spectra were collected in CDCl_3 or $\text{DMSO-}d_6$ at 25°C by using a Bruker 400 Hz spectrometer. Chemical shifts were reported in parts per million relative to internal standard tetramethylsilane ($\text{Si}(\text{CH}_3)_4 = 0.00$ ppm) or residual solvent peaks ($\text{CDCl}_3 = 7.26$ ppm, $\text{DMSO-}d_6 = 2.50$ ppm). ^1H NMR coupling constants (J) were reported in Hertz (Hz) and multiplicity was indicated as follows: s (singlet), d (doublet), t (triplet), q (quartet), and m (multiplet). Absorption spectra were collected by SynergyHTX microplate reader or a Shimadzu UV-3600 UV-Vis-NIR spectrophotometer. Photoluminescent spectra were captured by a HITACHI F4600 fluorescence spectrophotometer (excitation slit width was 5 nm and emission slit width was 10 nm). The operating environment of all the measurements was at room temperature. The image acquisition equipment was Zeiss LSM880 NLO (2 + 1 with BIG) Confocal Microscope System, which was equipped with objective LD C-Apochromat 63×1.15 W Corr M27, cell incubator with temperature control resolution $\pm 0.1^\circ\text{C}$, 405 nm Diode laser, Argon ion laser (458, 488 and 514 nm), HeNe laser (543 and 594 nm), and a Rack LSM 880 incl. 633 nm laser, with eight channels AOTF for simultaneous control of eight laser lines. Images processing was equipped with Zeiss User PC Advanced for LSM system (BLUE). A PMT detector was used for steady-state fluorescence, ranging from 420 to 700 nm. To collect the signals in 8-bit unsigned 1024×1024 pixels at a scan speed of 200 Hz, internal photomultiplier tubes were adopted.

2.2. Synthesis and characterization

2.2.1. Synthesis of compound CB

4-(diethylamino)salicylaldehyde (1.93 g, 10 mmol), 4-(bromomethyl)benzenboronic (2.97 g, 10 mmol) and K_2CO_3 (1.39 g, 10 mmol) were added in 20 mL tetrahydrofuran solution in a 100 mL three-neck flask. The mixture was refluxed for 12 h under N_2 . Then, the solution was extracted into ethyl acetate (3×75 mL). Then the solvent was evaporated *in vacuo* and the organic layer was combined. The residue was purified by silica column (petroleum ether/ethyl acetate = 5/1) to afford **CB** as white powders (4.13 g, yield: 73%). ^1H NMR (400 MHz, CDCl_3): δ 10.23 (s, 1H), 7.81 (d, $J = 8.1$ Hz, 2H),

7.71 (d, $J = 8.0$ Hz, 1H), 7.43 (d, $J = 8.1$ Hz, 2H), 6.27 (d, $J = 8.0$ Hz, 1H), 6.04 (s, 1H), 5.17 (s, 2H), 3.34 (q, 4H), 1.33 (s, 12H), 1.13 (t, 6H). ^{13}C NMR (100 MHz, CDCl_3): δ 187.2, 163.2, 153.7, 139.8, 135.3, 130.5, 126.3, 114.6, 104.7, 94.2, 83.9, 70.1, 44.9, 24.9 and 12.6.

2.2.2. Synthesis of probe CBH

Compounds **CB** (200 mg, 0.5 mmol), benzothiazole-2-acetonitrile (100 mg, 0.6 mmol) and 3 drop piperidine were added to 50 mL flask with 10 mL EtOH. Then, the mixture was refluxed for 3 h under N_2 . The reaction mixture was cooled to room temperature and filtrated. The residue was washed three times by cold EtOH and dried *in vacuo* to give compound CBH as yellow powders (146 mg, yield: 86 %). ^1H NMR (400 MHz, $\text{DMSO-}d_6$): δ 8.60 (s, 1H), 8.43 (d, $J = 8.8$ Hz, 1H), 8.01 (d, $J = 8.2$ Hz, 1H), 7.86–7.83 (m, 3H), 7.48–7.43 (m, 3H), 7.33 (t, 1H), 7.34 (dd, $J_1 = 9.2$ Hz $J_2 = 2.3$ Hz 1H), 6.05 (d, $J = 2.3$ Hz, 1H), 5.22 (s, 2H), 3.35 (q, 4H), 1.35 (s, 12H), 1.14 (t, 6H). ^{13}C NMR (100 MHz, $\text{DMSO-}d_6$): δ 166.0, 160.4, 154.0, 152.6, 141.2, 139.9, 135.3, 134.4, 130.6, 126.4, 126.1, 124.9, 123.0, 121.4, 118.7, 110.1, 105.4, 96.6, 94.9, 84.0, 70.5, 44.9, 29.8, 24.9, 12.7.

2.3. Preparation of the test solutions

Stock solutions of CBH (5 mM) were produced from dimethylsulfoxide (DMSO). Stock solutions of ROS, anions, cations, and amino acids were prepared using deionized water at a concentration of 100 mM. PBS buffer with 10% DMSO (pH = 7.4) solution were used to prepare test solutions. Absorption and fluorescence spectra were recorded when the test solutions were incubated for 30 min at room temperature.

2.4. Cytotoxicity determined by MTT method

HeLa cells were cultured in Dulbecco's modified Eagle medium (DMEM) containing 10% fetal bovine serum (FBS), 100 mg/L streptomycin, and 100 IU/mL penicillin, at 37°C in 5% $\text{CO}_2/95\%$ air incubator. The cytotoxicity of the probe was determined by using the MTT colorimetric cell proliferation kit (Roche), according to the manufacturer's guidelines. Firstly, HeLa cells were

cultured to 70–80% confluence in 96-well plates. The medium was aspirated and then replaced with 100 μL various concentrations of probe (10, 20, 30, 40 and 50 μM). Probes were employed from DMSO stocks while DMSO should not exceed 0.1% in the final solution. The same quantity of DMSO was also used as a negative control. After a total treatment for 24 h, the probe-containing medium was replaced with fresh DMEM medium without probes, and then MTT (50 μL , 1 mg/mL) was added to each well at 37°C in a 5% CO_2 /95% air incubator, reacting for 4 h. Optical densities measurements were followed by the manufacturer reference.

2.5. Cell imaging

Employing the probe monitoring exogenous H_2O_2 of HeLa cells, cells were controlled to grow to 60–70% confluence through seeded in glass-bottomed dishes. After incubating with 5 μM H_2O_2 and 10 μM H_2O_2 for 2 h, respectively, the old medium was replaced with fresh medium containing probe (2 μM) then cultured for 1 h. The cells were analyzed by imaging measurement after being washed with PBS buffer three times.

We employed the probe to monitor endogenous H_2O_2 of HeLa cells, which was further verified by the anti-oxidative effect of N-acetyl-cysteine (NAC). Cells grew to 60–70% confluence through seeded in glass-bottomed dishes. For two Rotenone-treated groups, cells were incubated with 5 μM Rotenone and 10 μM Rotenone for 1 h, respectively. Then, the old medium was replaced by the fresh medium containing probe (2 μM) then cultured for 1 h. For the NAC group, after incubating with 10 μM Rotenone for 1 h, HeLa cells were cultured with 5 and 10 μM NAC for 2 h, respectively. Then, the old medium was removed and a fresh medium containing probe (2 μM) were added to continue incubating for 1 h. All these cells were subjected to imaging analysis after being washed with PBS buffer three times.

The values of background signals of all images were nearly zero by imaging the same cells treated with the negative control (DMSO). All images were acquired on Zeiss LSM880 NLO (2 + 1 with BIG) Confocal Microscope System and the images processing were equipped with Zeiss User PC Advanced for LSM system (BLUE). Cell confocal images of probe employed an excitation filter of 488 nm and

the range of collective wavelength was between 510 and 650 nm.

2.6. Zebrafish imaging

5-day-old zebrafishes were used to detect exogenous and endogenous H_2O_2 . The fish was firstly anesthetized before imaging, which was imprisoned by using 0.01–0.02% tricaine in egg water. The zebrafishes were incubated with CBH (10 μM) for 2 h. Then, 100 μM H_2O_2 were added to the medium. After being washed by PBS, the zebrafishes were used for imaging. Endogenous H_2O_2 of zebrafish was induced by the anti-oxidative effect of NAC. By exciting the probe with 488 nm laser in optical windows between 510–650 nm, we could obtain the fluorescence images of zebrafishes.

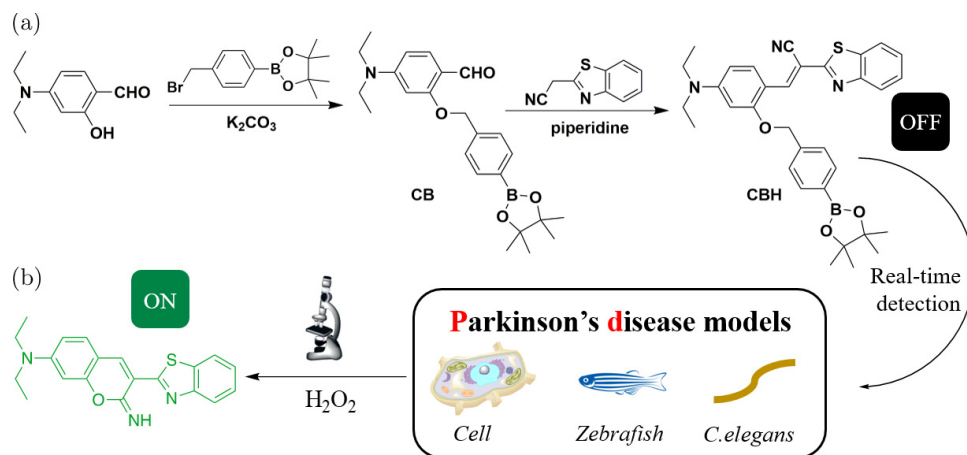
2.7. *C. elegans* imaging

N2 (wild type strain) and VC1024 (pdr-1 strain) worms were used and purchased from Caenorhabditis Genetics Center (University of Minnesota, USA), cultured at 15°C on nematode growth medium (NGM), and seeded with the uracil auxotroph strain, OP.50 of *E. coli*.

To detect H_2O_2 in different categories of *C. elegans*, we collected all the *C. elegans* that grew to young adults together at first and then divided them into four groups. Control group employed VC1024 worms to be immersed in PBS buffer (pH = 7.4) which contained only 1% DMSO for 5 min. For the N2 group, worms were treated with PBS buffer (pH = 7.4) included 10 μM probe for the same time. Both VC1024 group and NAC group utilized VC1024 worms that incubated with 10 μM probe for 5 min. *C. elegans* in NAC group were cultured in NGM including 10 μM NAC from the period L1 to young adults.

After worms were immersed in PBS buffers, respectively, they were transferred into NGM without *E. coli* and continued to be cultured at 15°C for 2 h, fixed into 2% agar padded slides before imaging.

The values of background signals of all images were close to zero by imaging the same worms treated with a negative control (DMSO). All images were acquired on Zeiss LSM880 NLO (2 + 1 with BIG) Confocal Microscope System and processed with Zeiss User PC Advanced for LSM system (BLUE). *C. elegans* images came from confocal



Scheme 1. (a) The design and synthesis route of the probe CBH; (b) Overall detection strategy by using probe CBH. The probe was used for bioimaging of H_2O_2 *in vitro*, in living HeLa cells, zebrafish and *C.elegans*.

microscope with an excitation filter of 488 nm and the collection wavelengths were from 510 to 650 nm.

3. Results and Discussion

3.1. Design and synthesis

As shown in Scheme 1, CBH was obtained by a simple and efficient way. Firstly, 4-(diethylamino)salicylaldehyde reacted with 4-(bromomethyl)phenylboronic acid pinacol ester in the presence of K_2CO_3 to give the intermediate **CB**. Then, **CB** was coupled with benzothiazole-2-acetonitrile by Knoevenagel condensation reaction to achieve the target probe CBH in a good yield. The phenylboronic acid group could be oxidized to phenol after reacting with H_2O_2 . The benzylphenol was eliminated and the cyclization

reaction was occurred to give dye with high conjugation that induced the enhanced emission. The structures of all the compounds were characterized by ^1H and ^{13}C NMR.

3.2. Response to hydrogen peroxide

The photophysical properties of CBH for H_2O_2 in PBS solution (containing 10% DMSO, pH = 7.4) were firstly evaluated. CBH showed a broad absorption band, ranging from 400 to 550 nm. A distinct increase in the absorption was observed when H_2O_2 was added and the concentration was increased from 0 to $600 \mu\text{M}$ (60 equiv.) (Fig. S1). This result suggested that the borate group could be oxidized by H_2O_2 , accompanied by C–O bond cleavage and releasing to give larger conjugated

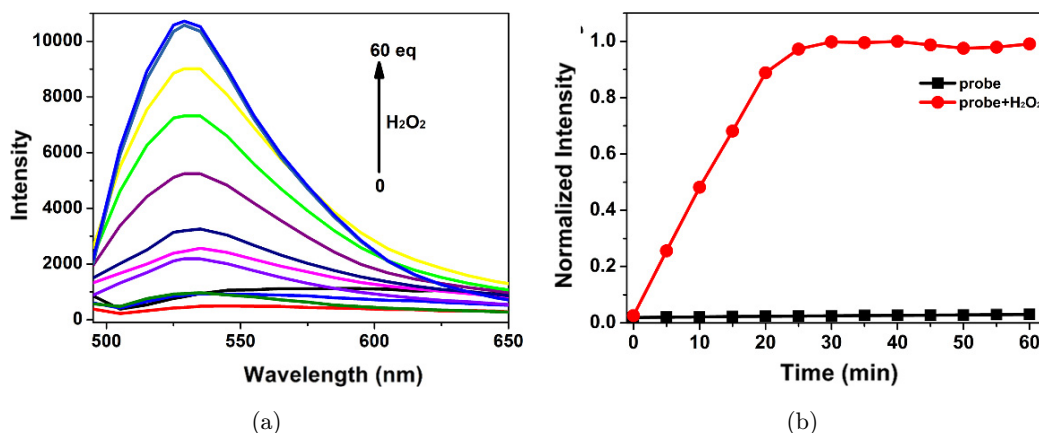


Fig. 1. (a) Fluorescence spectra of CBH in PBS buffer solution in the presence of H_2O_2 at different concentrations. (b) Time-dependent fluorescence intensity of CBH upon addition of 10 equiv. H_2O_2 in PBS buffer solution.

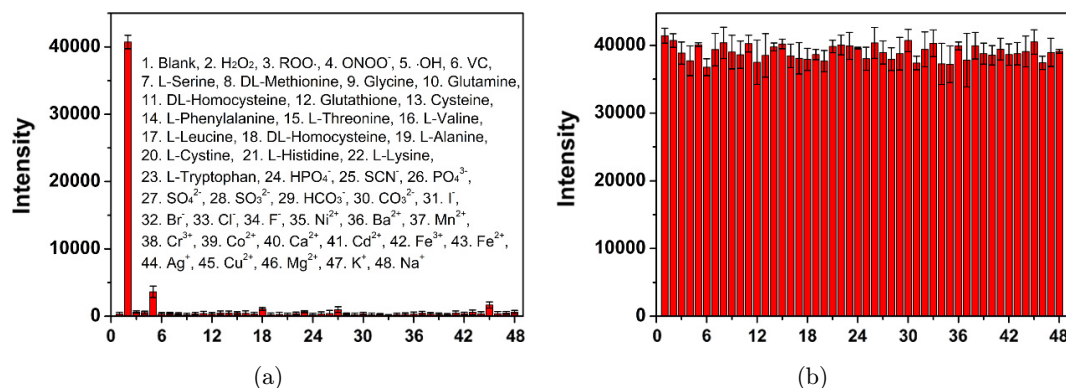


Fig. 2. (a) The fluorescence response of CBH in PBS buffer solution to various analytes. (b) The effect of various analytes on the fluorescence response of CBH in PBS buffer solution.

fluorophore. Meanwhile, it should be noted that the fluorescence intensity of CBH was quite weak at 600 nm in PBS solution (containing 10% DMSO, pH = 7.4). However, after the addition of H₂O₂, the fluorescence peak was blue-shifted from 600 to 530 nm and accompanied by dramatically enhanced intensity (Fig. 1). The fluorescence intensity at 530 nm increased about 12-fold by adding H₂O₂ from 0 to 60 equiv. The emission intensity at 530 nm increased linearly according to the concentration increase of H₂O₂, implying the great potential of CBH to quantify H₂O₂ (Fig. S2). The calculation value of the detection limit of CBH was as low as 0.72 μM. Moreover, the dynamics of the reaction of CBH with H₂O₂ were further investigated. As shown in Fig. 1(b), the time-dependent intensity at 530 nm increased rapidly and linearly upon the addition of H₂O₂ (10 equiv.) within 30 min. This result indicated the high sensitivity response of CBH to H₂O₂.

The fluorescence may be influenced by anions, cations as well as amino acids in living cells, as soon as the probes were applied in a complex biochemical environment. The selectivity of the probes should be investigated regardless of the influence of the various interferents. The effects on the fluorescence of the probes by more than 45 relevant biological species were also explored, including various normal anions, cations, amino acids and so on. As shown in Fig. 2(a), there are obvious fluorescence enhancement of CBH solution after the addition of 10 equiv. H₂O₂. Adding other ROS/RNS, anions, cations as well as amino acids to the solution of CBH, the fluorescence intensity of the probes showed negligible changes. Meanwhile, the effect of various analytes on the fluorescence response of CBH was also

investigated. As shown in Fig. 2(b), the addition of various analytes to the CBH solution with H₂O₂ did not induce any obvious changes in the emission intensity. The response of the probes to H₂O₂ was not affected by the various corresponding biological species. These results further confirmed that the probe had great potential for applying to the detection of H₂O₂ change in complex physiological environments.

3.3. Imaging

To evaluate whether CBH was useful for bioimaging application to detect H₂O₂ in living systems, the

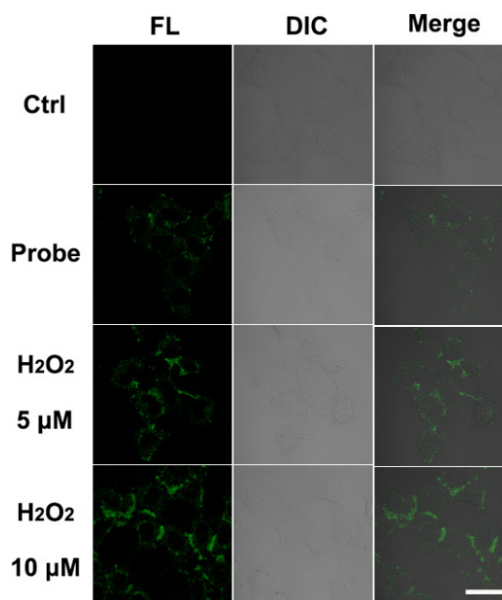


Fig. 3. Confocal fluorescence microscopy imaging of live HeLa cells pre-treated with CBH and different concentrations of H₂O₂ for 30 min at 37°C. Scale bar represents 20 μm.

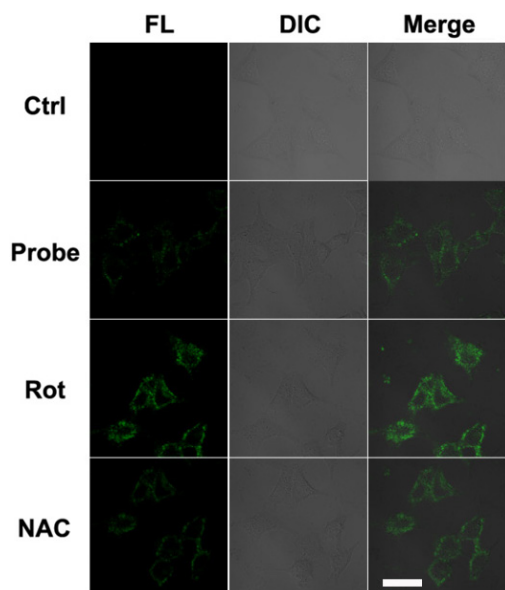


Fig. 4. Confocal images of HeLa cells incubated with CBH for 30 min with pretreatment of Rot and NAC. Scale bar represents 20 μm .

standard MTT assay was performed before imaging. The result showed that the cytotoxicity of CBH was negligible, even at the high concentration of 50 μM (Fig. S3). Based on the data above, we concluded that CBH could be applied for real-time monitoring of H_2O_2 in living systems, and act as a promising molecular imaging agent at the same time, to explore the biological activity of H_2O_2 under pathological conditions.

Fluorescence imaging was further used to evaluate the ability of the probe CBH on detecting the change of intracellular H_2O_2 . The HeLa cells were incubated with CBH at 37°C for 30 min firstly. As shown in Fig. 3, a weak fluorescence appeared. When the probe-loaded cells were treated with H_2O_2 , relatively strong fluorescence signals were detected from CBH channel in the cell images with the increase of H_2O_2 concentrations from 5 to 10 μM . Therefore, this result also demonstrated that CBH could detect the original and exogenous H_2O_2 in living cells.

Furthermore, we used the Rotenone (Rot), a high-affinity inhibitor of complex I of the mitochondrial electron-transfer chain that was known to induce the generation of ROS *in vitro*, as the inductive agent to regulate the H_2O_2 concentrations in cells.^{36,37} Thus, Rot could enhance the intracellular H_2O_2 concentrations. As shown in Fig. 4, the HeLa cells showed weak fluorescence, as a result of only being incubated with the probe CBH. Surprisingly, if the cells were treated with Rot for 30 min in advance, an obvious boost in fluorescence intensity could be observed. Meanwhile, to confirm the CBH could detect additional H_2O_2 induced by Rot, N-acetylcysteine (NAC), a widely used antioxidant for H_2O_2 elimination, was employed. After the cells treated with NAC further incubated with CBH and Rot, the fluorescence signal was largely decreased comparing to the group incubated with CBH and Rot. This

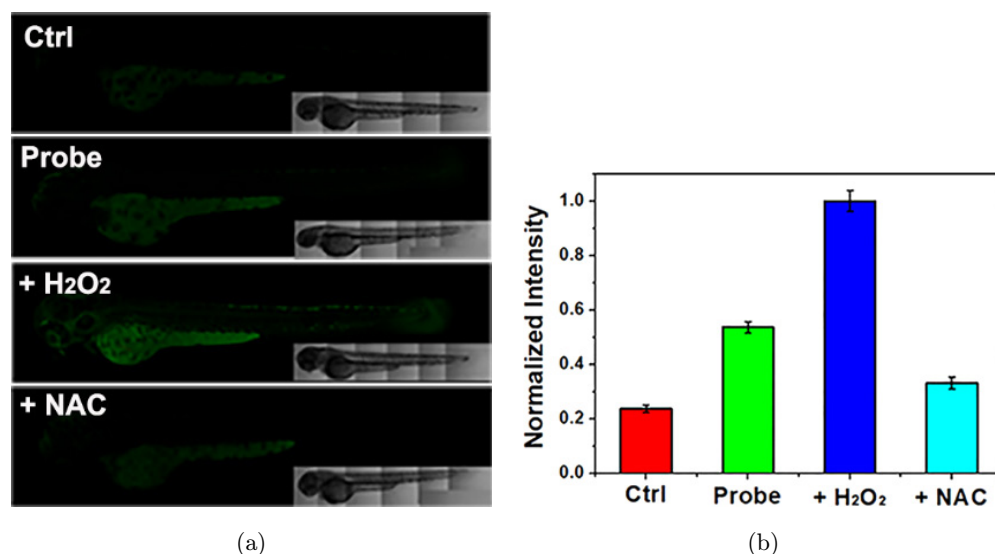


Fig. 5. (a) Confocal images of zebrafish (5-day-old) with CBH for 30 min and incubated with H_2O_2 or pretreated with NAC. (b) Relative fluorescence intensities of imaging.

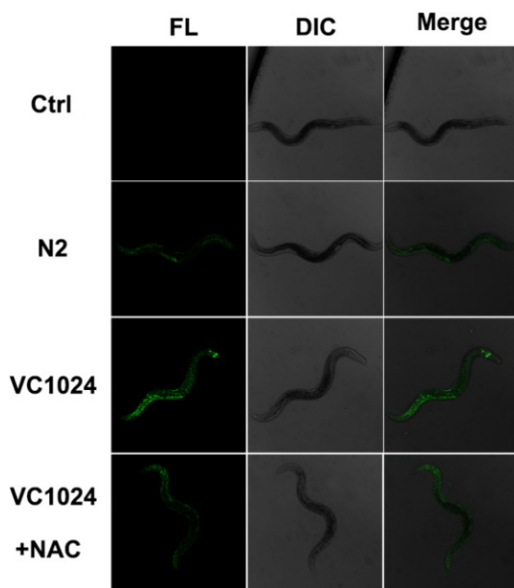


Fig. 6. Fluorescence imaging of N2 worms, normal VC1024 worms and VC1024 worms cultured with NAC, then incubated with CBH for 30 min at 37°C.

result further proved that CBH was able to detect the endogenous H_2O_2 induced by Rot.

The probe of CBH has been demonstrated to be capable for visualizing exogenous/endogenous H_2O_2 in mammalian cells. We provided a convenient means for rapid and sensitive detection of elevating levels of H_2O_2 to further assess whether CBH could be used in relevant tissue samples. The experiment of CBH on live zebrafish was performed. As shown in Fig. 5, there was very weak green fluorescence signal in zebrafish emitted from green fluorescent protein (GFP). After the zebrafish incubated with CBH up to 30 min, the fluorescence signal was slight increased due to the reaction of the probe and the endogenous H_2O_2 . When the zebrafish was pretreated by H_2O_2 and then incubated with CBH, an obvious fluorescence enhancement signal was detected. As for the zebrafish treated by NAC and further incubated with H_2O_2 , the fluorescence intensity using CBH imaging was decreased. It suggested that CBH had outstanding performance in relevant tissue samples imaging.

We next investigated the potential applications of the newly discovered H_2O_2 -specific imaging probe (CBH) for evaluating the relationship between H_2O_2 level and dopaminergic neuronal homeostasis in PD models. To realize this, we employed wild type strain N2 and VC1024 *C. elegans*, which had been established to exhibit PD-associated

phenotypes and excessive ROS production. As displayed in Fig. 6, there was no fluorescence signal of *C. elegans*. After the normal N2 worms treated by CBH, a weak fluorescence signal was observed. When the PD VC1024 worms were incubated with CBH for 30 min, a strong green fluorescence was detected. Furthermore, when the NAC pretreated VC1024 worms were incubated with CBH, there was an obvious decrease in fluorescence signal recorded comparing to the sample that was not treated by NAC. These results suggested that CBH had the capacity to precisely distinguish high levels of H_2O_2 in PD *elegans* model.

4. Conclusion

In conclusion, we had successfully developed a novel fluorogenic probe CBH for H_2O_2 detection in living organisms. The probes exhibited high sensitivity and selectivity to H_2O_2 . The fluorescence signals of the probe were weak in the PBS solution, but obviously enhanced in the presence of H_2O_2 and accompanied by the emission peak blue-shifted from 600 to 530 nm. Moreover, more than 45 various ROS/RNS, anions, cations and amino acids were involved and showed no effect on the response of CBH to H_2O_2 . The MTT assay showed CBH was low in toxicity. CBH was preferably adopted to detect the exogenous and endogenous H_2O_2 in cells and zebrafishes by fluorescence imaging due to its excellent sensing properties. More importantly, CBH had the capacity to precisely distinguish different levels of endogenous H_2O_2 in normal and PD *C. elegans* models. Thus, we expected the probe CBH might be developed to be a good boronate-based hydrogen peroxide probe for the early diagnosis of H_2O_2 related disease.

Conflict of Interest

The authors declare no conflicts of interest.

Acknowledgments

This work was financially supported by the National Natural Science Foundation of China (Grant Nos. 61905110 and 81672508), Jiangsu Provincial Foundation for Distinguished Young Scholars (BK20170041), China-Sweden Joint Mobility Project (51811530018), Natural Science Foundation of Shaanxi Province (2019JM-016)

and Fundamental Research Funds for the Central Universities.

Gaobin Zhang and Zheng Li contributed equally to this work.

References

1. B. D'Autreaux, M. B. Toledano, "ROS as signalling molecules: mechanisms that generate specificity in ROS homeostasis," *Nat. Rev. Mol. Cell Biol.* **8**(10), 813–824 (2007).
2. C. Nathan, A. Cunningham-Bussell, "Beyond oxidative stress: An immunologist's guide to reactive oxygen species," *Nat. Rev. Immunol.* **13**(5), 349–361 (2013).
3. D. Trachootham, J. Alexandre, P. Huang, "Targeting cancer cells by ROS-mediated mechanisms: A radical therapeutic approach?," *Nat. Rev. Drug Discov.* **8**(7), 579–591 (2009).
4. K. J. Barnham, C. L. Masters, A. I. Bush, "Neurodegenerative diseases and oxidative stress," *Nat. Rev. Drug Discov.* **3**(3), 205–214 (2004).
5. P. Fraisl, J. Aragonés, P. Carmeliet, "Inhibition of oxygen sensors as a therapeutic strategy for ischaemic and inflammatory disease," *Nat. Rev. Drug Discov.* **8**(2), 139–152 (2009).
6. B. Yang, Y. Chen, J. Shi, "Reactive oxygen species (ROS)-based nanomedicine," *Chem. Rev.* **119**(8), 4881–4985 (2019).
7. E. A. Veal, A. M. Day, B. A. Morgan, "Hydrogen peroxide sensing and signaling," *Mol. Cell* **26**(1), 1–14 (2007).
8. T. J. Collier, N. M. Kanaan, J. H. Kordower, "Ageing as a primary risk factor for Parkinson's disease: Evidence from studies of non-human primates," *Nat. Rev. Neurosci.* **12**(6), 359–366 (2011).
9. M. J. Devine, H. Plum-Favreau, N. W. Wood, "Parkinson's disease and cancer: Two wars, one front," *Nat. Rev. Cancer* **11**(11), 813–823 (2011).
10. J. K. Andersen, "Oxidative stress in neurodegeneration: Cause or consequence?," *Nat. Med.* **10**(S7), S18–S25 (2004).
11. J. Blesa, I. Trigo-Damas, A. Quiroga-Varela, V. R. Jackson-Lewis, "Oxidative stress and Parkinson's disease," *Front. Neuroanat.* **9**(91), 1–9 (2015).
12. Y. Yang, Q. Zhao, W. Feng, F. Li, "Luminescent chemodosimeters for bioimaging," *Chem. Rev.* **113**(1), 192–270 (2013).
13. J. L. Kolanowski, F. Liu, E. J. New, "Fluorescent probes for the simultaneous detection of multiple analytes in biology," *Chem. Soc. Rev.* **47**(1), 195–208 (2018).
14. K. Singh, A. M. Rotaru, A. A. Beharry, "Fluorescent chemosensors as future tools for cancer biology," *ACS Chem. Biol.* **13**(7), 1785–1798 (2018).
15. D. Wu, A. C. Sedgwick, T. Gunlaugsson, E. U. Akkaya, J. Yoon, T. D. James, "Fluorescent chemosensors: The past, present and future," *Chem. Soc. Rev.* **46**(23), 7105–7123 (2017).
16. G. Zhang, A. Ding, Y. Zhang, L. Yang, L. Kong, X. Zhang, X. Tao, Y. Tian, J. Yang, "Schiff base modified α -cyanostilbene derivative with aggregation-induced emission enhancement characteristics for Hg^{2+} detection," *Sens. Actuators B. Chem.* **202**, 209–216 (2014).
17. G. Zhang, X. Zhang, Y. Zhang, H. Wang, L. Kong, Y. Tian, X. Tao, H. Bi, J. Yang, "Design of turn-on fluorescent probe for effective detection of Hg^{2+} by combination of AIEE-active fluorophore and binding site," *Sens. Actuators B. Chem.* **221**, 730–739 (2015).
18. M. Abo, Y. Urano, K. Hanaoka, T. Terai, T. Komatsu, T. Nagano, "Development of a highly sensitive fluorescence probe for hydrogen peroxide," *J. Am. Chem. Soc.* **133**(27), 10629–10637 (2011).
19. Z. Song, R. T. Kwok, D. Ding, H. Nie, J. W. Lam, B. Liu, B. Z. Tang, "An AIE-active fluorescence turn-on bioprobe mediated by hydrogen-bonding interaction for highly sensitive detection of hydrogen peroxide and glucose," *Chem. Commun.* **52**(65), 10076–10079 (2016).
20. H. Xiao, P. Li, S. Zhang, W. Zhang, W. Zhang, B. Tang, "Simultaneous fluorescence visualization of mitochondrial hydrogen peroxide and zinc ions in live cells and in vivo," *Chem. Commun.* **52**(86), 12741–12744 (2016).
21. X. Chen, F. Wang, J. Y. Hyun, T. Wei, J. Qiang, X. Ren, I. Shin, J. Yoon, "Recent progress in the development of fluorescent, luminescent and colorimetric probes for detection of reactive oxygen and nitrogen species," *Chem. Soc. Rev.* **45**(10), 2976–3016 (2016).
22. M. Ren, B. Deng, K. Zhou, X. Kong, J.-Y. Wang, W. Lin, "Single fluorescent probe for dual-imaging viscosity and H_2O_2 in mitochondria with different fluorescence signals in living cells," *Anal. Chem.* **89**(1), 552–555 (2016).
23. B. Dong, X. Song, X. Kong, C. Wang, Y. Tang, Y. Liu, W. Lin, "Simultaneous near-infrared and two-photon in vivo imaging of H_2O_2 using a ratio-metric fluorescent probe based on the unique oxidative rearrangement of oxonium," *Adv. Mater.* **28**(39), 8755–8759 (2016).
24. H. Li, Q. Yao, J. Fan, J. Du, J. Wang, X. Peng, "A two-photon NIR-to-NIR fluorescent probe for imaging hydrogen peroxide in living cells," *Biosens. Bioelectron.* **94**, 536–543 (2017).
25. M. G. Savelieff, G. Nam, J. Kang, H. J. Lee, M. Lee, M. H. Lim, "Development of multifunctional molecules as potential therapeutic candidates for

- Alzheimer's disease, Parkinson's disease, and amyotrophic lateral sclerosis in the last decade," *Chem. Rev.* **119**(2), 1221–1322 (2019).
26. L. Qian, L. Li, S. Q. Yao, "Two-photon small molecule enzymatic probes," *Acc. Chem. Res.* **49**(4), 626–634 (2016).
 27. L. Wang, W. Du, Z. Hu, K. Uvdal, L. Li, W. Huang, "Hybrid rhodamine fluorophores in the visible/NIR region for biological imaging," *Angew. Chem. Int. Ed.* **58**, 14026–14043 (2019).
 28. G. Zhang, Y. Zhao, B. Peng, Z. Li, C. Xu, Y. Liu, C. Zhang, N. H. Voelcker, L. Li, W. Huang, "A fluorogenic probe based on chelation-hydrolysis-enhancement mechanism for visualizing Zn^{2+} in Parkinson's disease models," *J. Mater. Chem. B* **7**(14), 2252–2260 (2019).
 29. G. Zhang, Y. Ni, D. Zhang, H. Li, N. Wang, C. Yu, L. Li, W. Huang, "Rational design of NIR fluorescence probes for sensitive detection of viscosity in living cells," *Spectrochim. Acta. A Mol. Biomol. Spectrosc.* **214**, 339–347 (2019).
 30. X. Qiu, C. Xin, W. Qin, Z. Li, D. Zhang, G. Zhang, B. Peng, X. Han, C. Yu, L. Li, W. Huang, "A novel pyrimidine based deep-red fluorogenic probe for detecting hydrogen peroxide in Parkinson's disease models," *Talanta*. **199**, 628–633 (2019).
 31. X. Qin, C. Yu, J. Wei, L. Li, C. Zhang, Q. Wu, J. Liu, S. Q. Yao, W. Huang, "Rational design of nanocarriers for intracellular protein delivery," *Adv. Mater.* **31**(46), 1902791 (2019).
 32. H. Li, C. Xin, G. Zhang, X. Han, W. Qin, C. W. Zhang, C. Yu, S. Jing, L. Li, W. Huang, "A mitochondria-targeted two-photon fluorogenic probe for the dual-imaging of viscosity and H_2O_2 levels in Parkinson's disease models," *J. Mater. Chem. B* **7**(27), 4243–4251 (2019).
 33. Y. Liu, L. Bai, Y. Li, Y. Ni, C. Xin, C. Zhang, J. Liu, Z. Liu, L. Li, W. Huang, "Visualizing hydrogen peroxide in Parkinson's disease models via a ratiometric NIR fluorogenic probe," *Sens. Actuators B: Chem.* **279**, 38–43 (2019).
 34. T. W. Harris, "WormBase: A multi-species resource for nematode biology and genomics," *Nucleic Acids Res.* **32**(90001), 411D–417 (2004).
 35. M. Markaki, N. Tavernarakis, "Modeling human diseases in *Caenorhabditis elegans*," *Biotechnol. J.* **5**(12), 1261–1276 (2010).
 36. L. Li, C. W. Zhang, G. Y. Chen, B. Zhu, C. Chai, Q. H. Xu, E. K. Tan, Q. Zhu, K. L. Lim, S. Q. Yao, "A sensitive two-photon probe to selectively detect monoamine oxidase B activity in Parkinson's disease models," *Nat. Commun.* **5**, 3276 (2014).
 37. C. W. Zhang, H. B. Adeline, B. H. Chai, E. T. Hong, C. H. Ng, K. L. Lim, "Pharmacological or genetic activation of Hsp70 protects against loss of parkin function," *Neurodegener Dis.* **16**(5–6), 304–316 (2016).